Point-Spread Function Methods for Evaluating Display Reflection

John Penczek*, Michael E. Becker, Dirk Hertel*****
*University of Colorado, Boulder CO, USA
** Display-Messtechnik & Systeme, Rottenburg am Neckar, Germany
*** E Ink Corporation, Billerica MA, USA

Abstract
The point spread function method successfully separates specular and diffuse components of reflected glare from displays, with excellent agreement to previously reported annulus source and goniometric BRDF methods. Extracting haze profiles enables the prediction of ambient contrast with viewing direction. Of the three reflection components, haze has the greatest impact.

Author Keywords
Point spread function, bidirectional reflectance distribution function, specular reflectance, reflectance factor, display reflection, light scattering, unwanted reflections, haze.

1. Objective and Background
Ambient light reflections from the surface and within the top layer stack of a display are always unwanted, causing glare that distracts and yields visual discomfort. Unwanted reflections from emissive displays compete with the information-carrying emission; in reflective displays they compete with the information carrying reflection. Reflection mitigation includes antireflective coatings, scattering anti-glare (AG) surfaces, and reducing reflection and scatter in each stack component such as touch panels and frontlight sheets. Accurate measurement of unwanted reflection is critical for optimizing displays for minimum glare, avoiding contrast loss.

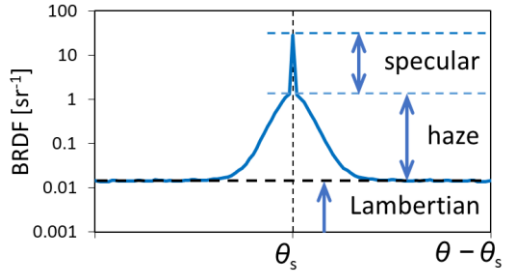

Figure 1. In-plane BRDF for a surface exhibiting specular, Lambertian, and haze light scattering components.

Kelley et al. used a three-component model to characterize the light reflected from a display.[1] Luminance reflected in the specular direction is composed by some combination of up to three possible reflection components: (1) uniform Lambertian scatter, (2) regular or specular (unscattered) Fresnel reflection, and (3) haze consisting of non-uniform scatter about the specular direction. When all three components are present for a given display structure, they can be identified by measuring the high-resolution bidirectional reflectance distribution function (BRDF). As shown by the example in Figure 1, the total reflected luminance in the specular direction is the superposition of all three reflected components. The Lambertian and haze components are both considered diffuse scatter since each redistribute light away from the specular direction.

Kelley proposed an alternative concept of measuring the specular reflectance component by using an annulus light source.[1] This method demonstrated the separation of specular and diffuse reflection components in the specular viewing direction for both reflective and emissive displays, resulting in its inclusion in the ICDM IDMS standard (section 11.7.3.2).[2-6] Extending the above work, Becker showed how a point light source and an imaging light measuring device (LMD) yielded the reflected point spread function (PSF) response of a surface.[7] This not only allowed separation of the specular component from diffuse scatter but also demonstrated the new capability of providing 2D haze profiles of surfaces with asymmetric scatter. In contrast, Kelley's annulus source method delivers the three reflection components only in the specular direction, and the in-plane BRDF is only a 1D cross-section of the 2D scatter profile.

This study first compares the PSF method to the BRDF and annulus source methods for several reflective and emissive surfaces. It then demonstrates the capability of the PSF method to extract haze reflectance factor profiles. These are subsequently used to predict ambient contrast profiles for emissive and reflective display samples under outdoor and indoor illumination conditions.

2. Experimental
Reflection characteristics measured by different methods are compared: in-plane BRDF, annulus, and PSF using standard (SDR) and high dynamic range (HDR) cameras.

2.1. In-plane BRDF
The in-plane BRDF measurement follows the converging beam method described in ASTM E2387-05.[8]

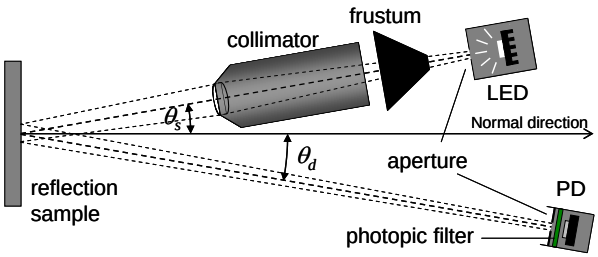

Figure 2. Schematic of the BRDF setup with converging beam and a photopic photodiode.

The previously described high-resolution apparatus shown in Figure 2 has a high-intensity white light emitting diode (LED) as a light source, photodiode (PD) with a photopic V(λ) filter as detector, and separate rotation stages for sample and source.[6] On passing through a circular aperture of 1 mm diameter, LED light is focused by a collimator lens onto a 3 mm diameter detector aperture. The diameter of the source aperture's specular image slightly underfills the detector aperture, resulting in a system angular resolution of 0.14°. The detector stayed at 5° inclination to the sample surface normal while the source rotates opposite to the inclination plane.

ISSN 0097-996X/25/5601-0393-$1.00 © 2025

2.2. Annulus Source method

The previously described annulus source method uses an integrating sphere light source of at least 99% uniformity (Keltek, LLC).[2-5] Annular sample illumination occurs as diffuse light exits a circular aperture subtending 1° from the sample surface, with a circular center stop subtending 0.33° (Figure 3).

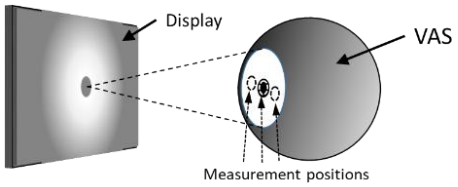

Figure 3. Annulus method with measuring positions.

Specular reflectance and haze are measured in a 15°/15° specular configuration, and Lambertian scatter is measured in a 45°/0° geometry. The light measuring device (LMD) can be an imaging photometer/colorimeter, or a spot photometer/spectroradiometer set to a measurement field angle of 0.1°. The LMD is focused on the center of the source aperture plane.

Reflected luminance is measured at the three positions shown in Figure 3. The center stop, obscuring direct (specular) light, only receives scattered light from Lambertian and haze reflection. The luminance in the annular area is the total of specular plus scattered reflected light. The reflected specular luminance component can be isolated by subtracting the center luminance from the reflected annular luminance, while the reflected haze luminance is isolated by subsequently subtracting the luminance of Lambertian scatter. A series of source aperture faceplates between 1° and 15° combines the annulus with the variable aperture source (VAS) method, yielding the source size dependence of reflected haze.[2-5]

2.3. Point Spread Function

The PSF implementation from three laboratories is compared in Table 1. The HDR imaging photometers/colorimeters are factory calibrated; the SDR CMOS color camera requires exposure bracketing and luminance calibration vs. a calibrated CS-2000 spectroradiometer.

Table 1. Specifications of the PSF measurements.

Laboratory	Lab 1	Lab 2	Lab 3
Light source	VAS with LEDs	Integrating sphere	LED + aperture
Source subtense	0.065° to 5°	0.11°	0.05°
Imaging LMD	Allied Vision 14bit b/w (Sony)	TechnoTeam LMK 6-12	Thorlabs CS126CU
Image sensor	⅓", 1.3MP CCD	1.1", 12MP CMOS	
Lens	50mm		75mm
Field of view	4.8° x 3.6°	16° x 12°	11° x 8°
Resolution	0.004°/pixel		0.003°/pixel
Dynamic range	10^5:1, HDR		10^3:1, SDR
Calibration	Luminance	XYZ	Luminance
Specular	8°/8°	15°/15°	4.5°/4.5°
Off-specular	30° to 80°/8°	45°/0°	45°/0°
Source-DUT / DUT-LMD	500mm / 500mm		635mm / 584mm

The LMD obtains the source luminance either directly in an unfolded geometry, or in reflection using a specular black glass standard. The source illuminance incident on the sample is determined via a Lambertian diffuse white reflection standard that is large enough to fill the LMD field of view. The SDR camera employs bracketing with two exposure times: short for peak specular and haze luminance relative to the specular black glass standard; long for maps of haze reflectance factor relative to the Lambertian diffuse white reflection standard.

3. Results

Specular reflectance, haze reflectance factor and reflected luminance profiles were obtained using in-plane BRDF, annulus and PSF methods. Reflective samples included the three scattering samples with varied gloss values G129, G61 and G27, made from sheet glass with etched front and black lacquer-coated back surfaces (Dr. M. Becker, Display-Metrology & Systems, Germany). [5] Display samples included tablets with an emissive liquid crystal display (LCD) and an eReader with a reflective electrophoretic display (EPD). Each display had half of their native screen surface modified with an AG or a glossy cover sheet.[5]

3.1. Resolving the specular component

The angular subtense of the light source and the angular resolution of the LMD determine the ability of a method to resolve the three reflections components. For the in-plane BRDF it is the goniometer step size, and the convolution of the detector aperture and the illuminator aperture image on the detector plane. For the PSF, it is the source size and angular resolution of the imaging LMD.

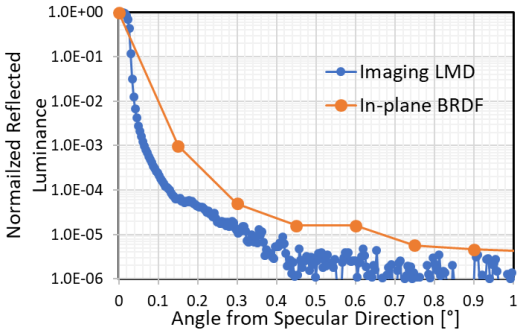

Figure 4. Normalized luminance profiles of a black glass sample, in-plane BRDF vs. PSF using an imaging LMD.

Figure 4 compares the system signature of the goniometric in-plane BRDF using the black glass sample to the PSF using an imaging LMD. This demonstrates each system's ability to resolve the ~0.1° reflected light source and its dynamic range. The imaging LMD has higher angular resolution and dynamic range.

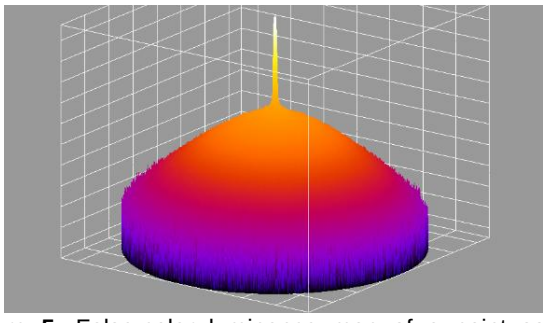

Figure 5. False-color luminance map of a point source reflected from the reflective sample G129, in logarithmic scale over six orders of magnitude and angles up to ±6º.

Using the PSF method, the specular reflectance of the three reflective samples with varied gloss were measured. The false-color luminance map shown in Figure 5 shows the reflected luminance distribution of the sample G129, with the specular reflectance peak rising above the haze hill. A luminance cross-section through this peak will produce a scatter profile similar to

that shown in Figure 1. The differential luminance between the peak's tip and base on the haze hill relative to the light source luminance gives the magnitude of the specular reflectance ζ_s.

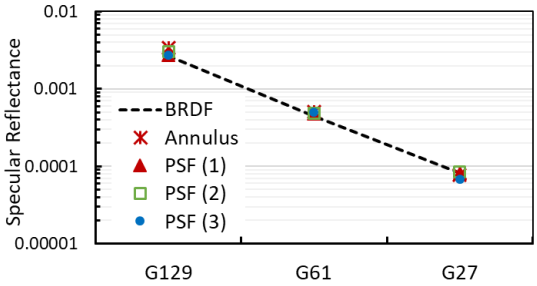

Figure 6. Comparison of specular reflectance ζ_s from BRDF, annulus source, and three PSF methods for the reflective samples with varied gloss G129, G61 and G27.

Figure 6 compares the three different PSF setups from Table 1 with specular reflectance values from BRDF and annulus source measurements. Although the specular reflectance was measured at different inclination angles (4.5°/4.5° to 15°/15°, see Table 1), Fresnel reflection calculations suggest only small differences. The good agreement demonstrated in Figure 6 confirms this, not only between the three PSF setups (Table 1) but also between all three measurement methods (BRDF, annulus and PSF). Each method essentially obtains the specular component by subtraction of the diffuse component from the total reflected luminance in the specular direction (see Figure 1). Figure 6 indicates that the PSF systems had sufficient angular resolution and dynamic range to resolve the specular component.

3.2. Resolving the diffuse components

The Lambertian reflected component ρ_L is measured separately in an off-specular geometry to exclude all haze. Such measurements were previously specified. [6, 9] In an EPD with its Lambertian image-forming layer, $\rho_{L,Q}$ is measured for each displayed color state Q. The Lambertian component is assumed to be constant in all viewing directions θ about the specular direction θ_s.

The reflected luminance map of the Lambertian component is subtracted from the total luminance map (such as Figure 5) so the remaining luminance map contains only the specular and haze components. Since the specular peak is quite distinct from the haze hill in angular space, it too can be subtracted from the specular plus haze luminance map.

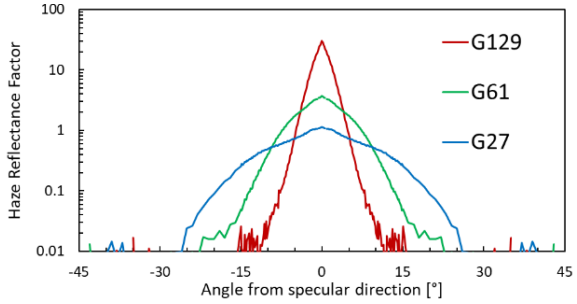

Figure 7. 1D profiles of haze reflectance factor $R_{H,\Psi}(\theta-\theta_s)$ for the reflective samples G129, G61 and G27 in the 15/15 configuration for a Ψ~0.1° point light source.

The resulting luminance map thus only contains the 2D haze contribution for the given illumination/detection geometry. The peak of the haze hill can be estimated from a Lorentzian fit. Figure 7 illustrates this, using a 1D luminance cross-section through the specular peak in Figure 5. Figure 8 shows good agreement of peak haze reflectance factors $R_{H,\Psi}(\theta-\theta_s)$ determined from the different measurement methods in the specular viewing direction.

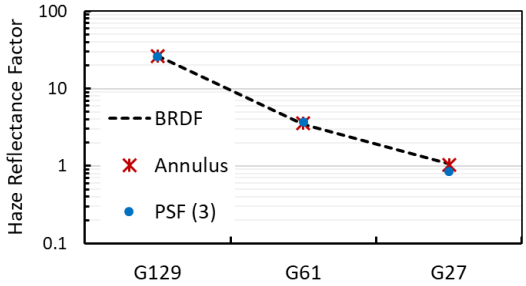

Figure 8. Comparison of haze reflectance factor from BRDF, annulus source, and PSF methods for G129, G61 and G27.

3.3. Predicting ambient contrast ratio

Light sources (sun, luminaires) that can cause unwanted reflection are specified by their subtense Ψ and luminance L_s, casting an illuminance E_s onto the display. The source distance is large so that E_s is uniform across the display. If such source causes a disturbing specular reflection off a display showing the color Q, then the angular distribution of luminance $L_Q(\theta-\theta_s)$ around the specular direction is composed of signal and noise components. In an emissive LCD, the signal is carried only by the emissive luminance $L_{Q,em}$; all reflective components are noise. In an EPD, the signal is carried by $\rho_{Q,L}$. The reflected Lambertian luminance is proportional to $\rho_{Q,L}$ and the total illuminance from the specular source E_s plus additional uniform background illumination E_d. The emissive and reflective signals are assumed constant with θ. The reflected noise consists of specular and haze components. The angular distribution of reflected specular luminance is simply the mirror image of the source, e.g. a top-hat distribution with luminance proportional to ζ_s and L_s, and width proportional to Ψ. The luminance distribution of haze from the reflection of an extended source of subtense Ψ depends on both E_s and Ψ. [4] The haze profile for an extended source $R_{H,\Psi}(\theta-\theta_s)$ can be determined from the haze distribution of a point source such as those shown in Figure 7 and Figure 9 by 1D-convolution. The angular distribution of display luminance $L_Q(\theta-\theta_s)$ around the specular direction can thus be expressed as sum of all emitted and reflected components: [9]

$$L_Q(\theta-\theta_s) = L_{Q,em} + \frac{\rho_{Q,L}(E_s+E_d)}{\pi} + \zeta_s \cdot L_s(\theta-\theta_s,\Psi) + \frac{R_{H,\Psi}(\theta-\theta_s)E_s}{\pi} \quad (1)$$

Once the luminance distributions $L_Q(\theta-\theta_s)$ are determined for the display colors Q = W (white) and Q = K (black), the angular distributions of ambient contrast ratio around the specular direction θ_s can be calculated as $CR(\theta-\theta_s) = L_W(\theta-\theta_s) / L_K(\theta-\theta_s)$.

Table 2 summarizes the measured reflection coefficients for the sample displays used to predict 1D distributions of display luminance around the direction of unwanted reflection.

Table 2. Reflection coefficients for the sample displays.

DUT	Tablet with LCD		eReader with EPD	
Surface	glossy (native)	AG	glossy	AG (native)
L_{em}(W)	320	285	0	0
L_{em}(K)	0.36	0.37	0	0
ρ_L(W)	0.0012	0.0039	0.45	0.43
ρ_L(K)	0.0009	0.0036	0.034	0.029
ζ_s	0.011	0.0017	0.055	0.0001
$R_{H,0}(0)$	11	32	54	20

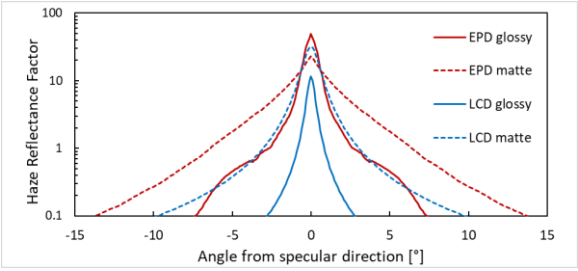

Figure 9. Point-source (Ψ~0.1°) 1D profiles of haze reflectance factor $R_{H,\Psi}(\theta-\theta_s)$ for the LCD and EPD samples.

Figure 9 shows the 1D profiles $R_{H,\Psi}(\theta-\theta_s)$ of haze surrounding a point light source reflected off the LCD and the EPD (each with their native and modified screens) after removing the specular and subtracting the Lambertian components. The EPD with its native AG surface has a wide haze distribution. Though modifying it with a glossy cover sheet narrows it (at the cost of a higher peak), this does not fully mitigate the internal scattering within the top layer stack. Even the LCD with its native glossy surface is not free of haze, caused by internal scatter and diffraction within the top layer stack. Modifying the LCD with a scattering AG cover sheet widens the haze distribution and increases its peak, most likely because the cover renders the antireflective coating ineffective.

Two application scenarios are explored using display data from Table 2, haze reflectance factor profiles from Figure 9, and Eq. (1). The point-source haze profiles were combined for larger sources up to 1° subtense by a 1D convolution approximation. [9]

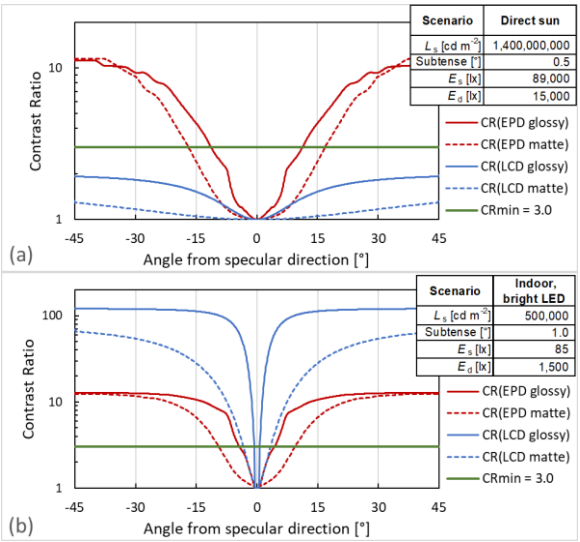

Figure 10. 1D profiles of Contrast Ratio (a) under outdoor sunlight and (b) in indoor illumination for LCD and EPD samples vs. a minimum threshold of 3.

The first scenario, Figure 10 (a), shows 1D profiles of contrast ratio surrounding an unwanted sun reflection under outdoor illumination. The sun's direct reflection at 1.4 10^9 cdm^{-2} incident from 15° inclination is disrupting the displayed information. The display is illuminated by 89 klx of direct sunlight plus 15 klx of hemispherical skylight. This hemispherical background illumination is useful to the EPD but severely reduces the LCD's off-specular contrast. The AG surface designed to reduce the intensity of reflected glare also spreads it to wider angles, thus increasing the angular range where CR is below a given threshold. For the LCD, haze from the AG cover sheet completely obliterates all information already impeded by reflected skylight. For the EPD, the glossy cover sheet does reduce the angular range of disturbing haze. The second scenario, Figure 10(b), models an indoor environment with 1,500 lx from off-specular task lighting plus diffuse background illumination, and unwanted reflection of a bright LED light of 500,000 cd m^{-2} subtending 1°. The hemispherical background illumination is responsible for reducing the LCD's off-specular contrast ratio to less than 50. For both LCD and EPD, the extended angular range of haze scatter increases the angular range where it disrupts display information.

Comparing the 1D profiles of CR in Figure 10 with the 1D haze distributions in Figure 9 suggests that haze scatter is the most disruptive unwanted reflection component, even for displays with glossy surfaces. Even small amounts of scatter and diffraction from sub-surface layer stack components can contribute significantly to haze, causing disruptive glare from unwanted reflection.

4. Impact

This study demonstrated that the PSF method compares well with the BRDF and annulus source methods for determining the specular reflectance of samples that exhibit significant diffuse scatter. There was also good agreement between the three PSF configurations, including the SDR camera with exposure bracketing. It was also shown how 1D and 2D profiles of the haze reflectance factor can be obtained by the PSF method. The ability to extract the haze profile from the other reflection components allows the prediction of ambient contrast ratio by viewing direction. This in turn allows quantitative prediction of how much of the displayed information would be impacted by a given illumination environment. Of the three reflection components, haze has the greatest impact.

5. References

1. Kelley, E.F, Jones, G.R., and Germer, T.A. (1998), Display Reflectance Model Based on the BRDF, Displays, 19, 27-34. DOI: 10.1016/S0141-9382(98)00028-6
2. Penczek, J., Kelley, E.F. and Smith, E. (2022), 39-2: Evaluating the Components of Reflected Glare in Displays. SID Digest, 53: 489-492. DOI: 10.1002/sdtp.15529
3. Penczek, J. (2024), 74-3: Regular Reflectance and Transmittance Measured by the Annulus Source Method. SID Digest, 55: 1015-1018. DOI: 10.1002/sdtp.17709
4. Hertel, D., Penczek, J. (2023), 18-1: Combining Annulus and Variable Aperture Source Methods to Separate Specular, Haze and Lambertian Reflection Components of ePaper Displays. SID Digest, 54: 221-224. DOI: 10.1002/sdtp.16530
5. Hertel, D., Penczek, J., Shin, J. (2024), 74-2: From BRDF to Gloss: Comparing Specular Reflectance Measurements. SID Digest, 55: 1011-1014. DOI: 10.1002/sdtp.17708
6. International Committee for Display Metrology (ICDM), *Information Display Measurements Standard* (IDMS), version 1.2 (2023), https://www.sid.org/Standards/ICDM.
7. Becker, M.E. (2005), Measurement and evaluation of display scattering. JSID, 13: 81-89. DOI: 10.1889/1.1867102
8. ASTM E2387-05: 2005 *Standard practice for goniometric optical scatter measurements*. DOI: 10.1520/E2387-05
9. Hertel, D. and Penczek, J. (2020), Evaluating Display Reflections in Reflective Displays and Beyond. Information Display, 36: 14-24. DOI: 10.1002/msid.1099